Calculation of rotational T_2 relaxation in solid parahydrogen and orthodeuterium

Marc Vanhimbeeck

Physics Department, University of Antwerp, Universiteitsplein 1, B-2610 Wilrijk, Belgium

Hans De Raedt*

Max-Planck-Institut für Physik und Astrophysik, Werner-Heisenberg-Institut für Physik, D-8000 München 40, Federal Republic of Germany

Ad Lagendijk

Natuurkundig Laboratorium, University of Amsterdam, Valckenierstraat 65, 1018 XE Amsterdam, The Netherlands

Dirk Schoemaker

Physics Department, University of Antwerp, Universiteitsplein 1, B-2610 Wilrijk, Belgium

(Received 17 June 1985)

The shifts, the relative intensities, and the linewidths of the rotational Raman spectrum of solid parahydrogen (p-H_2) and orthodeuterium (o-D_2) are calculated by combining the memory-function formalism and a second-order perturbation treatment of the electric-quadrupole–quadrupole interaction. Lattice vibrations are neglected in the present theory. The linewidth is shown to represent the phenomenological T_2-dephasing relaxation time, an upper bound of which can be set at ≈ 600 ps for p-H_2 and ≈ 100 ps for o-D_2. It is shown that at low pressure, the present theory compares favorably with the spontaneous Raman measurements on this solid.

I. INTRODUCTION

The study of vibrational and rotational relaxation phenomena in dense materials is receiving increasing attention. New impulses have come with the introduction of time resolved spectroscopy techniques on picosecond and subpicosecond time scales using mode-locked lasers. The general idea is to first excite the system via stimulated Raman scattering with a powerful laser pulse, after which a second pulse is used to probe the time evolution of the excitation. It is clear that this technique not only gives new dimensions to the study of fast relaxation processes, but that it also creates the need for theoretical calculations of the relaxation times to be expected. This is, however, not a straightforward matter because up to now the theoretical description of these experiments have treated the relaxation mechanism phenomenologically through the addition of exponential damping terms in the equations of motion for the collective amplitude (dephasing time T_2) and the excess population number (energy relaxation time T_1) of the excitation.[1] From a microscopic point of view, theoretical calculations on relaxation phenomena can be made within the framework of transport theory. It is therefore interesting to reformulate the phenomenological description in terms of this theory.

Within the framework of the electronic dipole approximation and linear optics, second-order time-dependent perturbation theory predicts that the spectral function $S_{PP}(\omega)$ of the scattered light be proportional to the Fourier transform of the polarization autocorrelation function $\langle P(0)P(t) \rangle$.[2] P stands for a component of the polarization tensor $\overline{P}$. With the use of the fluctuation-dissipation theorem one can connect the spectral function to the Laplace transformed polarization relaxation function $\Phi_{PP}(z)$,

$$S_{PP}(\omega) \sim \frac{-\omega}{1-e^{-\beta\omega}} \lim_{\epsilon\to 0} \mathrm{Im}\Phi_{PP}(\omega+i\epsilon) , \qquad (1.1a)$$

$$\Phi_{PP}(z) = \frac{\chi_{PP}(0)-\chi_{PP}(z)}{z} \qquad (1.1b)$$

in which $\chi_{PP}(z)$ is the polarization-polarization susceptibility. It is shown[2] that the spectral function $S_{PP}(\omega)$ for a damped harmonic oscillator with a periodic driving force is, in the vicinity of the resonance frequency ω_0, proportional to:

$$S_{PP}(\omega) \sim \frac{1/T_2}{(\omega-\omega_0)^2+(1/T_2)^2} , \qquad (1.2a)$$

or

$$S_{PP}(t) \sim e^{-t/T_2}\cos(\omega_0 t) , \qquad (1.2b)$$

which has led to the conclusion[1] that the homogeneous linewidth in spontaneous Raman measurements, and time-resolved studies of the coherent excitation, give the same T_2. This is of course under the assumption that the relaxation is well described by the phenomenological time T_2. As already mentioned, one can make calculations on the relaxation function (1.1b), and consequently by use of theorem (1.1a) determine a spectral function analogous to the one mentioned in (1.2a). If this result would strongly resemble (1.2a) then a T_2 time (in the sense of the phenomenological differential equations) could be identified. Great discrepancies on the other hand might indicate shortcomings in the phenomenological treatment.

We have made such calculations for rotational excitations in solid parahydrogen (p-H_2) and orthodeuterium (o-D_2) because a detailed and reliable description of the potentials in these solids is available. In the next section we will briefly discuss the model used to describe the rotational dynamics. In Sec. III we return to the subject of the polarization tensor and its expansion into operators, suitable for a description of rotational excitations. The actual calculation of the relaxation function is presented in Sec. IV and the results are discussed in Sec. V.

II. ROTATIONAL DYNAMICS IN THE SOLID

Solid hydrogen is a quantum solid which can be visualized as a collection of nearly-free quantum rotators whose centers of mass are, as a consequence of the large zero-point motion, not very sharply located on the hcp lattice sites of the crystal. Multiphonon relaxations in these solids have recently been shown to be relatively slow ($\simeq 10$ μs) (Ref. 3) in comparison with the pure rotational relaxations ($\simeq 100$ ps). We therefore restrict our attention to a description of the rotational motion without phonon cou-

pling. The Hamiltonian reads

$$H = H_0 + H_1 , \tag{2.1a}$$

with,

$$H_0 = \sum_i B J_i^2 , \tag{2.1b}$$

$$H_1 = \frac{1}{2} \sum_{i \neq j} A(\omega_i, \omega_j, R_{ij}) , \tag{2.1c}$$

H_0 representing the free quantum rotators (molecular angular momentum operator J_i) with molecular rotational constant $B = \hbar^2/2I$, and A_{ij} standing for the anisotropic interactions between the molecules i and j at distance R_{ij} and depending on their relative orientations ω_i, ω_j as expressed in a reference frame (ξ, η, ζ) with the ζ axes along the intermolecular axis $\mathbf{R}_{ij}$. As discussed by Van Kranendonk[4] it is a good approximation to restrict A to the long-range electric-quadrupole—quadrupole coupling (EQQ). After transforming the pair-tied frames (ξ, η, ζ) to a crystal-tied frame (x,y,z) with z axes along the hexagonal direction, the interaction Hamiltonian can be further specified as

$$H_1 = 2\pi\alpha_4 \sum_{i \neq j} \epsilon_4^{EQQ}(R_{ij}) \sum_{m,m'=-2}^{2} \left[\frac{4\pi}{9} \right]^{1/2} [Y_4^{m+m'}(\hat{R}_{ij})]^* C(224,mm') Y_2^m(\Omega_i) Y_2^{m'}(\Omega_j) , \tag{2.2a}$$

where

$$\epsilon_4^{EQQ}(R_{ij}) = \frac{Q_2(r_i)Q_2(r_j)}{5(R_{ij})^5} , \tag{2.2b}$$

$\alpha_4 = \sqrt{70}$, $C(l_1 l_2 l_3, m_1 m_2)$ stands for a Clebsch-Gordan coefficient,[5] and Y_l^m represents a spherical harmonic. Note the difference between the operators Y_2^m depending on the molecular orientations Ω in (x,y,z) and the functions Y_4^m depending on the orientation of the $\mathbf{R}_{ij}$ axis. The former will be considered as dynamical variables while the latter are merely numerical functions. Q_2 is the molecular quadrupole moment, depending on the internuclear distance r. The normalization is such that $\alpha_4 \epsilon_4^{EQQ}$ is a measure for the strength of the EQQ interaction. Since $\alpha_4 \epsilon_4^{EQQ}/B = 0.77$ for p-H_2 and 0.18 for o-D_2, one is allowed to treat H_1 perturbatively and to keep considering J as a nearly good quantum number for the solid. Note that the vibrational quantum number is not under consideration and as a result is assumed to retain its ground-state value $v=0$. Since the excitation energy of the state $J=4$ is $\simeq 1700$ K we will restrict ourselves to a two-level picture for the rotator ($J=0$ and $J=2$), resulting in six states: $|J=0, m=0\rangle$ and $|J=2, m\rangle$, $m = -2, \ldots, 2$.

It may be clarifying at this point to briefly summarize some results found by treating H_1 to first order:[4] (i) if the scattering region can be considered as small in comparison with the wavelength, only $\mathbf{k}=0$ states are excited in the Raman process, (ii) to first order in H_1, the Raman active $\mathbf{k}=0$ states form three equidistant levels corresponding to $m=0, \pm 1, \pm 2$, (iii) non-EQQ interactions make the separations slightly different, and (iv) within this formalism, the linewidth is zero.

III. ROTATIONAL RAMAN SPECTRUM

The spectral function determined in a Raman experiment is proportional to the Fourier transform of a polarization autocorrelation function $\langle P_{RS} P_{RS} \rangle$, RS denoting the Cartesian components of the crystal-polarization tensor $\bar{P}$ in the laboratory frame (X,Y,Z). It is our aim in the present section to show that, by properly transforming the Cartesian tensor components to their spherical components, the relevant part of $\langle P_{RS} P_{RS} \rangle$ can always be written as a linear combination of three simpler correlation functions.

Starting from (X,Y,Z), one can make a transformation to the lattice-tied frame (x,y,z), introduced previously by use of the direction cosines e_{rR} between the axes $\mathbf{e}_r$ and $\mathbf{e}_R$

$$P_{RS} = \sum_{rs} e_{rR} e_{sS} P_{rs} . \tag{3.1}$$

Working in the independent polarizability approximation,[4] the crystal polarization tensor $\bar{P}$ is given by

$$P_{rs} = \sum_{k=1}^{N} p_{rs}(\mathbf{r}_k) , \tag{3.2}$$

where $\bar{p}$ stands for the molecular polarization tensor, $\mathbf{r}_k = (r_k, \hat{\mathbf{r}}_k)$, $\hat{\mathbf{r}}_k$ denoting the orientation of the kth molecule in the reference frame (ξ_k, η_k, ζ_k) with ζ_k along the internuclear axis. For each such molecule, the Euler angles $(\alpha_k, \beta_k, \gamma_k)$ can be specified[5] to map (x,y,z) to (ξ_k, η_k, ζ_k). Then, the spherical tensor components, more suitable to treat the molecular orientations, are proportional to the isotropic and anisotropic parts p_i and p_a of

the tensor $\bar{p}$, defined by

$$\bar{p}=p_i \begin{bmatrix} 1 & 0 & 0 \\ 0 & 1 & 0 \\ 0 & 0 & 1 \end{bmatrix} + p_a \begin{bmatrix} -\frac{1}{3} & 0 & 0 \\ 0 & -\frac{1}{3} & 0 \\ 0 & 0 & \frac{2}{3} \end{bmatrix} . \qquad (3.3)$$

One finds

$$p_{RS}=p_{RS}^{(0)}+p_{RS}^{(2)} , \qquad (3.4a)$$

where

$$p_{RS}^{(0)}=-\sqrt{12\pi}p_i \sum_{mm'} \sum_{rs} e_{rR}e_{sS}(U_{mr})^*(U_{m's})^*C(110,mm'0)Y_0^0(\beta\alpha) , \qquad (3.4b)$$

and

$$p_{RS}^{(2)}=\sqrt{8\pi/15}p_a \sum_{\mu=-2}^{2} \sum_{mm'} \sum_{rs} e_{rR}e_{sS}(U_{mr})^*(U_{m's})^*C(112,mm'\mu)Y_0^0(\beta\alpha) , \qquad (3.4c)$$

where for simplicity we have suppressed the molecule index k. The U_{rs} are complex constants which appear when spherical components are introduced.[4] For evaluations of rotational Raman transitions, only $p_{RS}^{(2)}$ is relevant and it is not difficult to express this Hermitian operator as

$$p_{RS}^{(2)}=\sum_{\mu=0}^{2} p_{RS}^{(2,\mu)} , \qquad (3.5a)$$

with

$$p_{RS}^{(2,\mu)}=(1-\delta_{\mu0}/2)\sqrt{8\pi/15}p_a \sum_{mm'} \sum_{rs} e_{rR}e_{sS}C(112,mm'\mu)[(U_{mr})^*(U_{m's})^*Y_2^\mu+\text{c.c.}] . \qquad (3.5b)$$

When substituting this form in the correlation function $\langle p_{RS}^{(2)} p_{RS}^{(2)} \rangle$, many terms arise but with use of the selection rules given in Appendix B and after substitution of Eq. (3.2), it is possible to simplify the result to the form

$$\langle P_{RS}^{(2)} P_{RS}^{(2)} \rangle = \sum_{m=0}^{2} b_{RS}(m)\langle \mathscr{A}_2^m \mathscr{A}_2^m \rangle , \qquad (3.6)$$

where

$$\mathscr{A}_2^m = N^{-1/2} \sum_k [Y_2^m(k)+Y_2^{m*}(k)] .$$

The sum over k runs over all N lattice sites and clearly $\mathscr{A}_2^m$ is a $k=0$ Fourier transform. The coefficients $b_{RS}(m)$ are listed in Table I. The relative coefficients obtained from this list are identical to Van Kranendonk's results[4] with the exception of a factor of 2 for the values corresponding to $m=2$, which will be accounted for later on.

IV. CALCULATIONS

As explained in the preceding section, there are three spectral functions to be evaluated, corresponding to the three correlation functions $\langle \mathscr{A}_m \mathscr{A}_m \rangle$, $m=0,1,2$. In the following, we will omit the index "2." Using the fluctuation-dissipation theorem (1.1a) as a link between the spectral function $S_{\mathscr{A}_m \mathscr{A}_m}$ and the relaxation function $\Phi_{\mathscr{A}_m \mathscr{A}_m}$, we will concentrate on the latter, using the resolvent formalism and Kubo's scalar product[6]

$$\Phi_{AB}(z)= \left(A^\dagger, \frac{1}{z-L}B \right) , \qquad (4.1a)$$

$$(A,B)= \int_0^\beta d\lambda \langle A^\dagger e^{\lambda L}B \rangle , \qquad (4.1b)$$

$$\langle A \rangle = \text{Tr}(e^{-\beta H}A)/\text{Tr}\,e^{-\beta H} , \qquad (4.1c)$$

where the operators A and B represent physical observables and L is the Liouville operator that determines the operators' time evolution $(LA\equiv[H,A])$. From (4.1b) it follows that

$$(A,LB)=(LA,B)=\langle [A^\dagger,B] \rangle . \qquad (4.2)$$

In the following we will use L_0 and L_1 for the Liouville operators corresponding to H_0 and H_1, respectively. Note that we have $L_1\mathscr{A}_m=0$ because Y operators mutu-

TABLE I. Expansion coefficients $b_{RS}(m)$ of $\langle P_{RS}^{(2)}P_{RS}^{(2)} \rangle$ in units $2\pi p_a^2/45$.

| IJ | c\|\|Z | | Powder | | |
	$m=1$	$m=2$	$m=0$	$m=1$	$m=2$	$m=0$
XY	0	3	0	$\frac{6}{5}$	$\frac{6}{5}$	$\frac{3}{10}$
XZ	3	0	0	$\frac{6}{5}$	$\frac{6}{5}$	$\frac{3}{10}$
YZ	3	0	0	$\frac{6}{5}$	$\frac{6}{5}$	$\frac{3}{10}$
YY	0	3	$\frac{1}{2}$	$\frac{8}{5}$	$\frac{8}{5}$	$\frac{4}{10}$

ally commute. The relaxation function is determined using Mori's continued fraction formula[6] up to the fourth moment since this is the smallest possible form which actually introduces widths in the spectral function. The continued fraction is truncated using the procedure given in Ref. 7. The result of all this is as follows:

$$\Phi_{\mathscr{A}_m \mathscr{A}_m}(z) = \frac{(\mathscr{A}_m, \mathscr{A}_m)}{z - \dfrac{\Delta_1^2}{z + \Sigma_1(z)}} ,$$ (4.3a)

in which

$$\Sigma_1(z) = \frac{-\Delta_2^2}{z + i\kappa(\Delta_1^2 + \Delta_2^2)^{1/2}} ,$$ (4.3b)

$$\Delta_1^2 = \frac{\langle \omega^2 \rangle}{\langle \omega^0 \rangle} ,$$ (4.3c)

$$\Delta_2^2 = \frac{\langle \omega^4 \rangle}{\langle \omega^2 \rangle} - \frac{\langle \omega^2 \rangle}{\langle \omega^0 \rangle} ,$$ (4.3d)

$$\langle \omega^0 \rangle = (\mathscr{A}_m, \mathscr{A}_m) ,$$ (4.3e)

$$\langle \omega^2 \rangle = (L\mathscr{A}_m, L\mathscr{A}_m) ,$$ (4.3f)

$$\langle \omega^4 \rangle = (L^2\mathscr{A}_m, L^2\mathscr{A}_m) .$$ (4.3g)

According to Ref. 7 $\kappa = 1$, but since the approximation on Σ_1 is the most uncertain part in the calculation, we initially wanted to keep an extra degree of freedom, not changing the z dependence. Actually it turns out that $\kappa = 1$ gives the best agreement with the experimental results. Note that if $\Delta_2^2 = 0$, (4.3a) reduces to a sum of δ peaks at frequencies $\pm \Delta_1^2$. Within approximation (4.3) the linewidth therefore vanishes with vanishing Δ_2^2. Substituting (4.3a) and (4.3b) into (1.1a), one finds as the spectral function:

$$S_{\mathscr{A}_m \mathscr{A}_m} \sim \frac{\omega}{1 - e^{-\beta\omega}}$$

$$\times \frac{\langle \omega^0 \rangle \Delta_1^2 \Delta_2^2 (\Delta_1^2 + \Delta_2^2)^{1/2}}{[\omega^3 - \omega(\Delta_1^2 + \Delta_2^2)]^2 + \kappa^2(\Delta_1^2 + \Delta_2^2)(\omega^2 - \Delta_1^2)^2} .$$ (4.4)

Using the formulas in Appendix B it can be shown that

$$(\mathscr{A}_0, \mathscr{A}_0) = 2(\mathscr{A}_1, \mathscr{A}_1) = 2(\mathscr{A}_2, \mathscr{A}_2) ,$$

which means that the m dependence of $\langle \omega^0 \rangle$ in the numerator renders precisely the factor of 2, mentioned at the end of the preceding section. Remember that the experimental measurements consist of linear combinations $(m = 0,1,2)$ of the functions (4.4) according to (3.6). The coefficients $b_{RS}(m)$ depend on the experimental setup and should be incorporated when comparing our theoretical results with experiment. In the vicinity of the rotational transitions $(\omega \simeq \Omega_0 = 512$ K for p-H_2 and 258 K for o-D_2), and at a characteristic temperature of 4.2 K $e^{-\beta\omega}$ is negligibly small (respectively, 10^{-53} and 10^{-27} for p-H_2 and o-D_2).

To calculate the moments (4.3e)–(4.3g), one can start from the definition (4.1b). That is what we intend to do for $\langle \omega^0 \rangle$, but the other moments can be simplified using (4.2) so that we have to calculate explicitly

$$\langle \omega^0 \rangle = \int_0^\beta d\lambda \, \text{Tr}(e^{(-\beta + \lambda)H} \mathscr{A}_m e^{-\lambda H} \mathscr{A}_m) ,$$ (4.5a)

$$\langle \omega^2 \rangle = \text{Tr}(e^{-\beta H}[\mathscr{A}_m, L_0 \mathscr{A}_m]) ,$$ (4.5b)

$$\langle \omega^4 \rangle = \text{Tr}(e^{-\beta H}[L_0^2 \mathscr{A}_m, L_0 \mathscr{A}_m])$$
$$+ \text{Tr}(e^{-\beta H}[L_1 L_0 \mathscr{A}_m, L_0 \mathscr{A}_m]) .$$ (4.5c)

Since we know first-order calculations yield a sum of δ functions,[4] it is expected that the first nonzero contributions to Δ_2^2 can only appear from second-order on. Equations (4.5) will therefore have to be evaluated up to second order in the EQQ interaction according to the following perturbation formula:

$$e^{-\beta(H_0 + \lambda H_1)} = e^{-\beta H_0} - \lambda \int_0^\beta d\tau \, e^{(\tau - \beta)H_0} H_1 e^{-\tau H_0} + \lambda^2 \int_0^\beta d\tau \int_0^\tau d\tau' e^{(\tau - \beta)H_0} H_1 e^{(\tau' - \tau)H_0} H_1 e^{-\tau' H_0} + O(\lambda^3) .$$ (4.6)

Further simplification of (4.5c) is possible if one realizes that H_0 describes a two-level system with time evolution L_0. Confining ourselves to the $|J = 0, m = 0\rangle$, $|J = 2, m\rangle$, $m = -2, \ldots, 2$ subspace, one verifies that the matrix representation of Y_m satisfies

$$e^{(iL_0 t)} Y_m = \cos(t\Omega_0) Y_m + \frac{i}{\Omega_0} \sin(t\Omega_0) L_0 Y_m + Z_m .$$ (4.7)

This implies that in the time correlation function, there will be a time-independent contribution, and hence Z_m can be identified as a nonergodic part of the matrix representation of Y_m. Since this part is known, it is possible to correct for it. However, an analytical evaluation of $[Y_m, \exp(iL_0 t) Y_m]$ up to first order in EQQ reveals that its contributions to the moments (4.5) are proportional to the Boltzmann factor $\exp(-\beta \Omega_0)$ which is perfectly negligible. It is therefore allowed to use the relation $L_0^2 Y_m = \Omega_0^2 Y_m$ and further simplify (4.5) to

$$\langle \omega^0 \rangle = 2 \sum_i \int_0^\beta d\lambda \langle e^{\lambda H} Y_m(i) e^{-\lambda H} Y_m(0) \rangle \delta_{m,0} + (-1)^m \sum_i \int_0^\beta d\lambda \langle e^{\lambda H} Y_m(i) e^{-\lambda H} Y_{-m}(0) \rangle ,$$ (4.8a)

$$\langle \omega^2 \rangle = 2\{ \langle [Y_m(0), L_0 Y_m(0)] \rangle \delta_{m,0} + (-1)^m \langle [Y_{-m}(0), L_0 Y_m(0)] \rangle \} ,$$ (4.8b)

$$\langle \omega^4 \rangle = 2\Omega_0^2 \{ \langle [Y_m(0), L_0 Y_m(0)] \rangle \delta_{m,0} + (-1)^m \langle [Y_{-m}(0), L_0 Y_m(0)] \rangle \}$$

$$+ 2 \sum_i \{ \langle [L_1 L_0 Y_m(i), L_0 Y_m(0)] \rangle \delta_{m,0} + (-1)^m \langle [L_1 L_0 Y_{-m}(i), L_0, Y_m(0)] \rangle \} .$$ (4.8c)

TABLE II. Number of different terms appearing in the analytical evaluation of the elementary constituents of (4.8) up to second order in the EQQ interaction.

	Zeroth order			First order			Second order		
	$m=1$	$m=2$	$m=0$	$m=1$	$m=2$	$m=0$	$m=1$	$m=2$	$m=0$
(Y_m, Y_m)	1	1	1	1	1	1	75	66	59
$\langle (Y_m, L_0 Y_m) \rangle$	1	3	2				40	120	80
$\langle (L_1 L_0 Y_m, L_0 Y_m) \rangle$				1	6	3	128	268	119

A sum over i means that a lattice sum runs over all lattice sites, and the number "0" indicates a fixed lattice point, which can be chosen as origin. The factors $\delta_{m,0}$ follow from the m-selection rule given in Appendix B stating that the sum of the m values should equal zero. Deriving these Kronecker δ's is somewhat more subtle than might appear at first sight and includes lattice symmetry considerations. The problem is that in the perturbation expansion each H_1 contributes two extra Y_m operators whose m values are to be considered as well.

As already mentioned, evaluations with pen and paper have been done up to first order but extension to second order was quite hopeless. We therefore turned to the computer-program COMMUT (Ref. 8) which handles the analytic evaluations of the commutators in (4.8) using the algebra of the angular momentum operators J^+, J^-, and J^z and the operators Y_m. An additional procedure was written to evaluate the operators $e^{-\beta H}$ perturbatively to second order. To evaluate the traces, resolutions of the identity $\sum | Y_l^m \rangle \langle Y_l^m | = 1$ ($l = 0,2$ and $m = -l,..,l$) have been inserted whenever it was necessary. This results in three types of matrix elements,

$$\langle Y_l^m | Y_2^M | Y_l^m \rangle ,$$

$$\langle Y_l^m | Y_2^M Y_2^{M'} | Y_l^m \rangle ,$$

and

$$\langle Y_l^m | Y_2^M Y_2^{M'} Y_2^{M''} | Y_l^m \rangle ,$$

which can all be expressed in terms of Clebsch-Gordan coefficients as indicated in Appendix A. All these analytical manipulations have been carried out on a VAX 11/780 computer, resulting in 977 different contributions, divided over the possible cases as given in Table II.

V. RESULTS

Printing all these terms here would make the paper too long and we therefore will restrict ourselves to the numerical evaluation of $\langle \omega^2 \rangle / \langle \omega^0 \rangle$ and $\langle \omega^4 \rangle / \langle \omega^2 \rangle$ since they immediately lead to Δ_1^2 and Δ_2^2. In Table III results for $T = 4.2$ K are given in the form

$$\Lambda_0 [1 + \Lambda_1 (\epsilon_4^{EQQ}/B) + \Lambda_2 (\epsilon_4^{EQQ}/B)^2] , \qquad (5.1)$$

Λ_0, Λ_1, and Λ_2 resulting from zeroth-, first-, and second-order calculations, respectively. Λ_0 is expressed in units $(6B)^2$. The temperature dependence (in the region 0–12

K) of the coefficients Λ_i is negligible as expected from previous considerations on the Boltzmann factor. As a consequence, slight differences in the numerical value of B have no effect on Λ_i and only influence Δ_1^2 and Δ_2^2 as explicitly given by (5.1). This is also illustrated by the fact that, within the numerical accuracy of our calculations, we found the same values of Λ_i for p-H_2 as for o-D_2. In further calculations we will use the zero-pressure values[9] $B = 85.379$ (43.040) K and $\epsilon_4^{EQQ} = 0.791$ (0.979) K. From now on, o-D_2 results will be mentioned between parentheses. Note that these values for ϵ_4^{EQQ} are not corrected for zero-point motions. The spectral function (4.4) at zero-pressure is shown in Fig. 1 and numerical evaluations of the peak positions, full width at half-maximum (FWHM), and relative intensities are listed in Table IV. It follows that the splitting of the signals is given by

$$\delta_{(2-1)} = 2.475 \; (3.050) \; cm^{-1} ,$$

$$\delta_{(0-2)} = 2.458 \; (3.000) \; cm^{-1} .$$

High precision measurements give 2.01 ± 0.01 (2.6 ± 0.1) cm^{-1} and 1.98 ± 0.01 (2.6 ± 0.1) cm^{-1}, respectively.[10] As we have already mentioned, the first nonvanishing contributions to Δ_2^2 are of second order in EQQ. Consequently, the continued fraction (4.3a) can be approximated up to first order by setting $\Sigma_1 = 0$, resulting in two equally separated δ peaks. The values for the first-order splitting obtained in this way are consistent with the ones of Van Kranendonk's first-order perturbation treatment of the Hamiltonian (2.1). On the other hand, we do not know if our approximation (4.3b) on Σ_1 contains all second-order

TABLE III. Coefficients Λ_0, Λ_1, and Λ_2 [see (5.1)]. Λ_1 and Λ_2 are dimensionless numbers and Λ_0 is expressed in units $(6B)^2$. Since the temperature dependence of the Λ_i is negligible in the region from 0 to 12 K, our results depend only on the parameters ϵ_4^{EQQ} and B as explicitly given by (5.1) and apply to both p-H_2 and o-D_2.

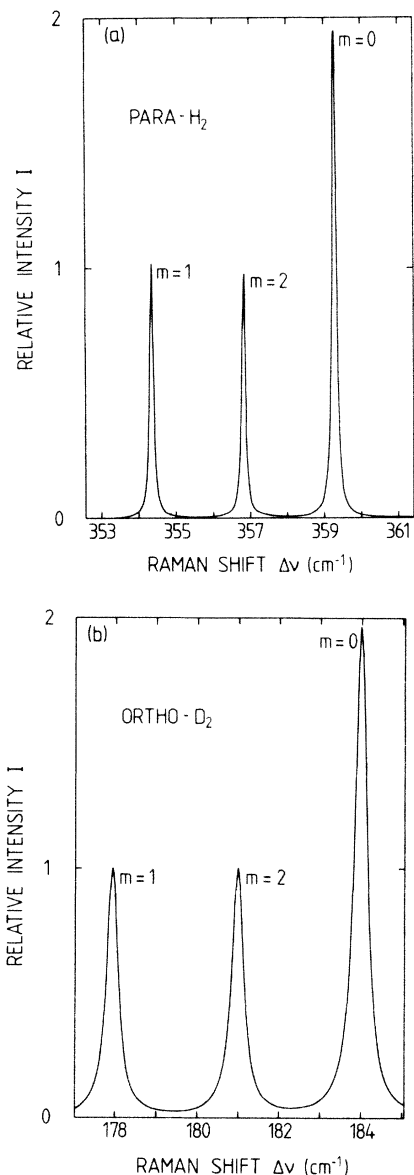|		Λ_0	Λ_1	Λ_2
$\langle \omega^2 \rangle / \langle \omega^0 \rangle$	$m=0$	1	1.8035	14.7702
	$m=1$	1	-1.2023	15.9265
	$m=2$	1	0.3006	15.3461
$\langle \omega^4 \rangle / \langle \omega^2 \rangle$	$m=0$	1	1.8035	22.6357
	$m=1$	1	-1.2023	23.1819
	$m=2$	1	0.3006	22.9069

FIG. 1. Spectral functions $S_{\mathscr{A}_m\mathscr{A}_m}$ (a) for p-H_2 and (b) for the o-D_2, for the zero-pressure values of the parameters Δ_1^2 and Δ_2^2 listed in Table III. For comparison with an experimental situation, remember to include the coefficients $b_{RS}(m)$ as indicated by Table I.

contributions. Therefore, the line splittings presented in this work do not necessarily have to agree with those of a second-order perturbation calculation on (2.1).[11]

Our calculations introduce a FWHM of 0.11 (0.35) cm^{-1} while the experiment mentioned above gives a value of 0.3 ± 0.1 (1 ± 0.1) cm^{-1}. The resolution of the experiment was 0.1 cm^{-1} and a convolution of (4.4) with a Gaussian of width $\sigma=0.05$ $\sqrt{2\ln2}$ cm^{-1} increases the FWHM from 0.11 (0.35) cm^{-1} to 0.17 (0.41) cm^{-1}. Very likely, part of the discrepancy is due to inhomogeneous broadening.

To calculate a time scale from this width, one can determine the inverse Laplace transform of (4.1a). This

TABLE IV. Properties of the zero-pressure spectral function at $T=4.2$ K. The transition frequency (Ω_0) and full width at half-maximum (FWHM) are given in cm^{-1}. The intensities $(\mathscr{I})$ are normalized to the signal $m=2$.

	Ω_0	FWHM	$\mathscr{I}$
$m=1$ p-H_2	354.346	0.11	1.03
$m=2$ p-H_2	356.821	0.12	1.00
$m=0$ p-H_2	359.279	0.12	1.95
$m=1$ o-D_2	177.925	0.34	1.002
$m=2$ o-D_2	180.975	0.35	1.000
$m=0$ o-D_2	183.975	0.36	1.970

function then describes the time-dependent relaxation:

$$S(t)=\Upsilon e^{-t/\tau}\cos(\Omega_0 t)+\Upsilon' e^{-t/\tau}\sin(\Omega_0 t)+\Upsilon'' e^{-t/\tau'} .$$

$$(5.2)$$

The relaxation times and proportionality coefficients are listed in Table V. The excitation frequencies Ω_0 can be found in Table IV. It is clear from Table V that Υ' and Υ'' are sufficiently small to map (5.2) with the single exponential form (1.2b), from which τ can be identified with the dephasing time T_2. One should avoid the temptation to give any physical interpretation to the other time τ' in terms of T_1 or T_2. As a matter of fact, by increasing the number of poles in the relaxation function (4.3a) one could in principle increase the number of relaxation times in (5.2) up to any number. Note that the o-D_2 and p-H_2 results scale as

$$\frac{(T_2)_{\text{o-}D_2}}{(T_2)_{\text{p-}H_2}} \sim \left| \frac{(\epsilon_4^{EQQ}/B)_{\text{o-}D_2}}{(\epsilon_4^{EQQ}/B)_{\text{p-}H_2}} \right|^2 ,$$

as is expected from the second-order character of the phenomenon.

Via its R^{-5} dependence, the coupling constant ϵ_4^{EQQ} is strongly pressure dependent. In Fig. 2 we scanned the behavior of the excitation frequency and the widths of the signals as a function of V_0/V where V_0 is the zero-pressure volume and V is a value under pressure. At low pressure the results are in qualitative agreement with experiment,[12] but for higher values, great discrepancies with the experiment are seen. This can partly be understood from the knowledge that the EQQ Hamiltonian (2.2) is only valid for the long-range region of the intermolecular potential. On the other hand there is the increasing influence of phonon coupling at the higher pressures. Note that, as pressure increases, the calculated asymmetry in the splitting between the three signals remains too small in comparison with experiment, but that the low pressure splittings compare favorably, indicating the importance of second-order treatments of pairwise interactions.

The results of Fig. 2 can be fit with a fourth-order polynomial of the form

$$E(V_0/V)=\sigma_4(V_0/V)^4+\sigma_3(V_0/V)^3+\sigma_2(V_0/V)^2$$

$$+\sigma_1(V_0/V)^1+\sigma_0 ,$$

$$(5.3)$$

TABLE V. Coefficients Υ, Υ', and Υ'' and relaxation times τ and τ' of the time relaxation function (5.2). The relaxation times are expressed in ps and the numbers are normalized to Υ.

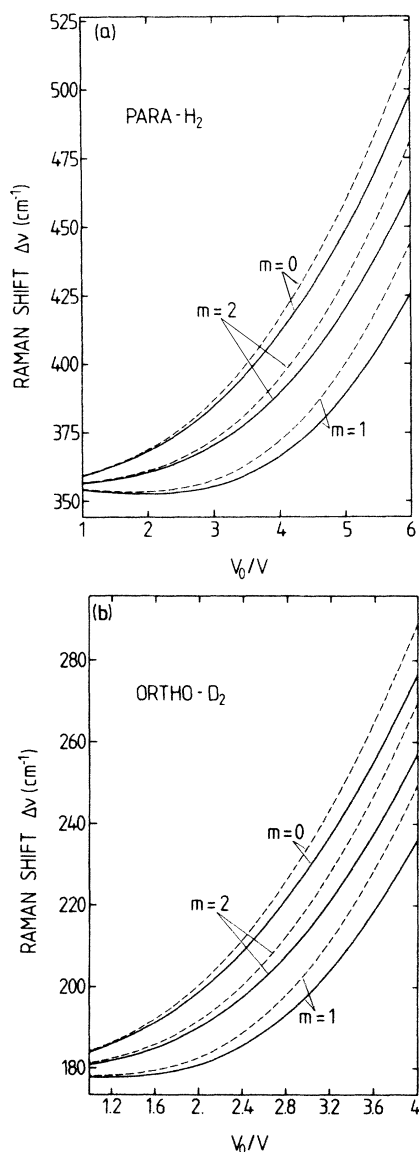|	Υ	Υ'	Υ''	τ	τ'
$m=1$ p-H_2	1.0	-1.6×10^{-3}	-3.1×10^{-4}	599.2	0.094 15
$m=2$ p-H_2	1.0	-1.6×10^{-3}	-3.1×10^{-4}	578.8	0.093 50
$m=0$ p-H_2	1.0	-1.7×10^{-3}	-3.3×10^{-4}	560.2	0.092 84
$m=1$ o-D_2	1.0	-9.4×10^{-3}	-1.9×10^{-3}	98.84	0.094 60
$m=2$ o-D_2	1.0	-9.6×10^{-3}	-1.9×10^{-3}	96.48	0.093 00
$m=0$ o-D_2	1.0	-9.6×10^{-3}	-1.9×10^{-3}	94.27	0.091 49

FIG. 2. Theoretical curves (a) for p-H_2 and (b) for the o-D_2 for the pressure dependence of the transition frequency Ω_0 (solid line) and the frequency $\Omega_0 + \text{FWHM}/2$ (dashed line) for the various signals ($m=1,2,0$). V_0 is the molecular volume under zero pressure and V stands for a pressurized value. These curves can well be fit with a fourth-order polynomial, the coefficients of which can be found in Table VI. The minimum in the curves for $m=1$ is reached for $V_0/V \simeq 2.07$ for p-H_2 and 1.2 for o-D_2.

within an error of at most 0.16 (0.20) cm^{-1}. The coefficients σ_i can be found in Table VI, as well as a set of coefficients σ'_i which reproduce the upper-limit lines in the figure. From the two curves one can determine the FWHM.

VI. CONCLUSION

We have calculated the Raman spectrum for the rotational transition $|J=0\rangle \rightarrow |J=2\rangle$ in solid p-H_2 and o-D_2. In setting up the model, we assumed that the EQQ interaction is responsible for the rotational relaxation. To calculate the Raman spectrum it is necessary to go beyond first-order perturbation theory. A second-order treatment not only introduces a relaxation time T_2 (a finite linewidth) but also changes the relative intensities and the splittings of the Raman lines when compared to the first-order theory. As the EQQ interaction changes with pressure, we have also studied the pressure dependence of the Raman spectrum. Up to a certain pressure qualitative agreement is good. For large pressures the theory breaks down. In nonpublished work[13] a compilation was made of experimental data (Raman and far infrared, both at low and high density) on deuterium and hydrogen. It turns out, and this may be against one's feeling, that the best fit to experiment was obtained by using a pure EQQ interaction. All attempts to include the more sophisticated non-EQQ components have given poor results. It is clear that this aspect is far from being understood.

ACKNOWLEDGMENTS

APPENDIX A: MATRIX ELEMENTS

Integrals of two spherical harmonics are defined by the orthogonality relation

$$\int \int d\Omega [Y_{l_1}^{m_1}(\Omega)]^* [Y_{l_2}^{m_2}(\Omega)] = \delta_{l_1 l_2} \delta_{m_1 m_2} , \qquad (A1)$$

TABLE VI. The fitting parameters σ_i (in cm^{-1}) for the calculated lines of Fig. 2 (at 4.2 K), according to formula (5.3). To obtain the peak positions Ω_0, use the rows labeled a; to obtain $\Omega_0 + W_{\text{FWHM}}/2$, use the rows labeled b. The polynomials fit our theoretical results within an error of at most 0.16 cm^{-1} for p-H$_2$ and 0.20 for o-D$_2$.

		σ_4	σ_3	σ_2	σ_1	σ_0
$m=0$	a	$-0.021\,6864$	$0.556\,9865$	$1.057\,6295$	$2.002\,7256$	355.7605
p-H$_2$	b	$-0.032\,4876$	$0.752\,550\,11$	$0.675\,6668$	$2.483\,9597$	355.5228
$m=1$	a	$-0.029\,3426$	$0.981\,0988$	$-3.025\,0537$	$0.960\,8626$	355.4955
p-H$_2$	b	$-0.042\,9154$	$1.227\,5625$	$-3.616\,8385$	$1.720\,0356$	355.1508
$m=2$	a	$-0.030\,6221$	$0.829\,1255$	$-1.168\,4549$	$1.790\,1521$	355.4418
p-H$_2$	b	$-0.047\,9620$	$1.121\,6729$	$-2.007\,9300$	$3.116\,1509$	354.6805
$m=0$	a	$-0.127\,8003$	$1.660\,3171$	$0.982\,0361$	$2.206\,3837$	179.2854
o-D$_2$	b	$-0.086\,8651$	$1.267\,3898$	$3.620\,0206$	$-2.200\,9168$	181.7010
$m=1$	a	$-0.156\,3892$	$2.608\,3207$	$-4.346\,1261$	$-0.109\,3836$	180.0385
o-D$_2$	b	$-0.194\,0767$	$3.003\,5689$	$-4.345\,2601$	$-0.838\,7852$	180.6256
$m=2$	a	$-0.052\,2367$	$1.173\,5765$	$1.995\,1739$	$-4.564\,8613$	182.6338
o-D$_2$	b	$-0.258\,7442$	$3.295\,9602$	$-4.399\,4031$	$4.594\,3117$	177.9115

whereas integrals of more than two functions on the same lattice site can always be reduced to the previous one by using the coupling rule for spherical harmonics

$$Y_{l_1}^{m_1}(\Omega)Y_{l_2}^{m_2}(\Omega) = \sum_l V(l_1 l_2 l)C(l_1 l_2 l, m_1 m_2)$$
$$\times C(l_1 l_2 l, 00)Y_l^{m_1 + m_2}(\Omega) , \quad \text{(A2)}$$

with

$$V(l_1 l_2 l_3) = \left[\frac{(2l_1+1)(2l_2+1)}{4\pi(2l_3+1)} \right]^{1/2} . \quad \text{(A3)}$$

From these basic formulas, one immediately finds

$$\langle Y_{l_3}^{m_3} | Y_{l_2}^{m_2} | Y_{l_1}^{m_1} \rangle = V(l_1 l_2 l_3)C(l_1 l_2 l_3, m_1 m_2)C(l_1 l_2 l_3, 00) , \quad \text{(A4)}$$

$$\langle Y_{l_4}^{m_4} | Y_{l_3}^{m_3} Y_{l_2}^{m_2} | Y_{l_1}^{m_1} \rangle = \sum_l V(l_1 l_2 l)V(l_3 l l_4)C(l_1 l_2 l, m_1 m_2)C(l_1 l_2 l, 00)C(l_3 l l_4, m_3 m_1 + m_2)C(l_3 l l_4, 00) , \quad \text{(A5)}$$

$$\langle Y_{l_5}^{m_5} | Y_{l_4}^{m_4} Y_{l_3}^{m_3} Y_{l_2}^{m_2} | Y_{l_1}^{m_1} \rangle = \sum_{l,k} V(l_1 l_2 l)V(l_3 lk)V(l_4 ll_5)C(l_1 l_2 l, m_1 m_2)C(l_1 l_2 l, 00)$$

$$\times C(l_3 lk, m_3 m_1 + m_2)C(l_3 lk, 00)C(l_4 kl_5, m_4 m_1 + m_2 + m_3)C(l_4 kl_5, 00) . \quad \text{(A6)}$$

APPENDIX B: SELECTION RULES

Characteristic for a perturbative approach is that one always considers energies of the unperturbed system which in this case only depend on l (0 or 2) but not on m $(-l, \ldots, l)$. Therefore, the matrix elements above always appear with a summation over m, directly resulting from the trace

$$\sum_{m=-l}^{l} \langle Y_l^m | Y_{l'}^{m'} | Y_l^m \rangle$$
$$= V(ll'l)C(ll'l, 00) \sum_{m=-l}^{l} C(ll'l, mm') . \quad \text{(B1)}$$

By including $C(l0l, m0) = 1$, the summation over m can be evaluated, using the orthogonality of the Clebsch-

Gordan coefficients, leading to

$$\sum_{m=-l}^{l} \langle Y_l^m | Y_{l'}^{m'} | Y_l^m \rangle = \frac{(2l+1)}{\sqrt{4\pi}} \delta_{m'0}\delta_{l'0} . \quad \text{(B2)}$$

We refer to this formula as the "l selection rule."

The previous considerations are only valid for a specific summation of matrix elements, but one can also make statements on the m values of single matrix elements, occurring in the evaluation of traces. Starting with the most elementary case $\langle Y_{l_1}^{m_1} | Y_l^m | Y_{l_1}^{m_1} \rangle$, the Wigner-Eckart theorem states $m=0$. This can be extended to combined forms

$$\langle Y_{l_1}^{m_1} | Y_l^m | Y_{l_2}^{m_2} \rangle \langle Y_{l_2}^{m_2} | Y_{l'}^{m'} | Y_{l_1}^{m_1} \rangle ,$$

leading to $m + m' = 0$. Finally formula (A2) also permits us to include matrix elements of combined operators; e.g.,

$$\langle Y_{l_1}^{m_1} | Y_l^m Y_{l'}^{m'} | Y_{l_2}^{m_2} \rangle \langle Y_{l_2}^{m_2} | Y_{l''}^{m''} | Y_{l_1}^{m_1} \rangle$$

is only nonvanishing for $m + m' + m'' = 0$. These results can be summarized by the statement that, whatever combination of operators one might have on a particular lattice site, the sum of their m values must be equal to zero. This rule is referred to as the "m selection rule."

---

*Permanent address: Physics Department, University of Antwerp, Universiteitsplein 1, B-2610 Wilrijk, Belgium.

[1] A. Lauberau and W. Kaiser, Rev. Mod. Phys. 50, 607 (1978).

[2] W. Hayes and R. Loudon, The Scattering of Light by Crystals (Wiley, New York, 1978).

[3] Chien-Yu Kuo, R. J. Kerl, N. D. Patel, and C. K. N. Patel, Phys. Rev. Lett. 53, 27 (1984).

[4] J. Van Kranendonk, Solid Hydrogen (Plenum, New York, 1983).

[5] M. E. Rose, Elementary Theory of Angular Momentum (Wiley, New York, 1967).

[6] D. Foster, Hydrodynamic Fluctuations, Broken Symmetry and Correlation Functions (Benjamin, Reading, Mass., 1975).

[7] H. De Raedt and B. De Raedt, Phys. Rev. B 15, 5379 (1971).

[8] H. De Raedt, J. Fivez, and B. De Raedt, Comput. Phys. Commun. 23, 209 (1982).

[9] I. F. Silvera, Rev. Mod. Phys. 52, 393 (1980).

[10] S. S. Bhatnagar, E. J. Allin, and H. L. Welsh, Can. J. Phys. 40, 9 (1962).

[11] J. I. Igarashi, J. Phys. Soc. Jpn. 53, 2629 (1984).

[12] I. F. Silvera and R. J. Wijngaarden, Phys. Rev. Lett. 47, 39 (1981).

[13] R. J. Wijngaarden, L. Lasse, V. Goldman, A. Lagendijk, and I. F. Silvera (unpublished).